

Emerging ideas on the molecular basis of protein and peptide aggregation

D Thirumalai*, DK Klimov and RI Dima

Several neurodegenerative diseases are associated with the unfolding and subsequent fibrillization of proteins. Although neither the assembly mechanism nor the atomic structures of the amyloid fibrils are known, recent experimental and computational studies suggest that a few general principles that govern protein aggregation may exist. Analysis of the results of several important recent studies has led to a set of tentative ideas concerning the oligomerization of proteins and peptides. General rules have been described that may be useful in predicting regions of known proteins (prions and transthyretin) that are susceptible to fluctuations, which give rise to structures that can aggregate by the nucleation-growth mechanism. Despite large variations in the sequence-dependent polymerization kinetics of several structurally unrelated proteins, there appear to be only a few plausible scenarios for protein and peptide aggregation.

Addresses

Institute for Physical Science and Technology, University of Maryland, College Park, Maryland 20742, USA
*e-mail: thirum@glue.umd.edu

Current Opinion in Structural Biology 2003, 13:XXX-XXX

This review comes from a themed issue on
Theory and simulation
Edited by Charles L Brooks III and David A Case

0959-440X/03/\$ – see front matter
© 2003 Elsevier Science Ltd. All rights reserved.

Abbreviations

ASA	accessible surface area
CD	circular dichroism
EM	electron microscopy
EPR	electron paramagnetic resonance
FTIR	Fourier transform IR
HB	hydrogen bond
MD	molecular dynamics
NCC	nucleated conformational conversion
OR ²	Oliveberg-Richardson-Richardson
PDB	Protein Data Bank
PHF	paired helical filament
PrP ^C	cellular form of prion protein
PrP ^{Sc}	pathogenic scrapie form of prion protein
R ²	Richardson and Richardson
SSE	secondary structure element
TTR	transthyretin

Introduction

A large number of neurodegenerative diseases, including Alzheimer's disease [1,2] and the transmissible prion disorders [3,4], are associated with amyloid fibrils. Historically, amyloid referred to the extracellular deposits that were thought to be the cause of various diseases [2,5]. Many recent studies have

found that mobile oligomers, which are precursors to fibril formation, may themselves be neurotoxic [2,6,7]. Several experiments have further shown that any generic protein, under suitable conditions, can form ordered aggregates, with morphologies that closely resemble the amyloid fibrils [8,9]. The finding that any protein can aggregate at high enough protein concentration and under suitable external conditions (pH, salt concentration, temperature) is not surprising. It is interesting, however, that even proteins and peptides that are not associated with known diseases form fibrils with the cross β -patterns that are characteristic of amyloid fibrils [9,10]. A more surprising finding is that the oligomers that form early in the aggregation process of even non-disease-related proteins may be cytotoxic [11]. The formation of morphologically similar aggregates by a variety of proteins unrelated in sequence or structure suggests that certain general principles may govern fibrillization [10,12–14]. The vastness of sequence space and the heterogeneity of environmentally dependent intermolecular interactions make deciphering the principles of protein aggregation difficult.

The polymerization of proteins and peptides raises several questions of biophysical interest. First, what are the early events in the oligomerization process? In particular, what is the nature of the structural fluctuations that trigger the association of polypeptide chains? Second, it has been established, beginning with the classic studies of gelation of deoxyhemoglobin S [15], that polymerization occurs by a nucleation and growth process [16]. Nevertheless, several questions remain unanswered. What are the structural characteristics of the critical nuclei? Is the formation of distinct strains [17–19] reflected in the nature of the critical nuclei? Third, can the sequence and/or the structural characteristics of monomers provide insights into the sites that harbor amyloidogenic tendencies? Fourth, what are the principles that natural proteins use in preventing aggregation under physiological conditions? Fifth, can the variations in the fibrillization rates of naturally occurring mutants (in prions, transthyretins [TTRs] and A β peptides) be related to the biophysical characteristics of the monomers?

It is beyond the scope of this review to describe our current understanding of all the questions posed above. Topics related to the first two questions have been described in recent excellent reviews [10,12,13]. The past few years have witnessed considerable progress on several fronts in the field of protein aggregation. Here, we outline a few of these, with the emphasis on biophysical aspects of fibrillization. Some of the highlights are:

102 1. Solid-state NMR studies [20,21^{**},22,23^{*}], imaging of
103 A β oligomers using atomic force microscopy (AFM) [24]
104 and cryo-EM [25,26] have been used to obtain insights
105 into the structural organization of amyloid fibrils. The
106 determination of A β fibril structures has led to
107 computational strategies [27^{*}] that distinguish between
108 different models of fibril structures.

109 2. Several reports, especially in the context of
110 Alzheimer's disease, have shown that the soluble
111 oligomers themselves, rather than the protease-resistant
112 plaque, may be the cause of neurotoxicity [2,6,7,28].
113 This finding has made it critical to understand the
114 kinetics of aggregation of protofibrils, which are the
115 precursors to the fibrils.

116 3. A detailed study of the fibrillization of A β peptides
117 and their congeners has shown that the formation of
118 fibrils with β -sheet architecture must involve the
119 transient population of α -helical structures [29^{**}].
120 Molecular dynamics (MD) simulations of the
121 oligomerization of A β ₁₆₋₂₂ peptides [30^{**}] further suggest
122 that, for this class of peptides, the formation of helical
123 structures may be an obligatory intermediate step.

124 4. Exploration of the sequence and structural
125 requirements needed to prevent fibrillization has given
126 insights into the plausible regions in the cellular
127 isoforms of prion proteins (PrP^c) and A β peptides that
128 may be implicated in the transition to the fibrillar form
129 [31^{**},32^{**}]. These computational studies have led to
130 testable predictions that are beginning to be confirmed
131 in experiments.

132 5. Systematic studies of natural β -sheet proteins have
133 led to the identification of the potential mechanisms
134 that block aggregation [33^{**}]. The translation of these
135 observations into a simple computational rule allows us
136 to predict regions that may be implicated in the
137 production of intermediates that can grow into fibrils.

138 The purpose of this review is to formulate tentative
139 ideas on the molecular origins of aggregation by
140 synthesizing these important developments. A survey of
141 seemingly unrelated studies suggests that a few
142 qualitative principles about protein aggregation can be
143 proposed. It is also clear that there are several
144 outstanding issues that can only be addressed using a
145 combination of experimental, theoretical and
146 computational techniques. The review concludes with a
147 description of a few of these outstanding problems.

148 **Conformational fluctuations of monomers** 149 **provide a limited glimpse into fibrillization**

150 It is known that aggregation kinetics depends on the
151 sequence and the precise external conditions.
152 Truncation of the two C-terminal residues of the A β
153 peptide, whose sequence using single-letter code for
154 amino acids is
155 DAEFRHDSG¹⁰YEVHHQKLVF²⁰FAEDVGSNKG³⁰AI
156 IGLMVG⁴⁰VIA, results in substantial differences in
157 the timescale of plaque formation for the A β ₁₋₄₀ and A β ₁₋
158 ₄₂ peptides [29^{**}]. It has also been shown that E22Q

159 ('Dutch') A β peptide has enhanced activity (as
160 measured by peptide deposition rates) relative to the
161 wild-type peptide for both the full-length (1-40)
162 peptide and truncated (10-35) variants [34,35].
163 Similarly, aggregation times, under similar external
164 conditions, vary greatly for wild-type TTR and its
165 naturally occurring mutants [36^{**}]. The difference in
166 amyloidogenic characteristics is observed both in the
167 rate of deposition of monomers onto existing fibrils and
168 in the kinetics of oligomerization of peptides.

169 The observation of sequence-dependent deposition
170 rates for A β peptides has been used to hypothesize that
171 variations in the rates of amyloidogenesis may be
172 explained by the propensity of different monomer
173 sequences to form local structure [37,38]. To assess the
174 validity of this hypothesis, Straub and co-workers
175 [39,40,41^{**}] have carried out a series of MD simulations
176 of the wild-type and Dutch mutant of A β ₁₀₋₃₅ peptide.
177 Surprisingly, the analysis of multiple 1 ns MD
178 simulations demonstrated that both peptides have very
179 similar conformational properties. There is no
180 appreciable difference in the β -structure propensities of
181 the two peptides. The results of these studies imply
182 that the structural characteristics of monomeric peptides
183 may not be indicative of their amyloidogenic
184 competence [39,40,41^{**}]. Because, in general, the
185 profound conformational changes are driven by
186 interpeptide interactions, it is unlikely that the
187 conformational dynamics of isolated peptides can fully
188 explain variations in deposition rates.

189 We have proposed two alternative explanations for the
190 change in the rate of amyloid formation between the
191 wild type and E22Q mutant [41^{**}]. Deletion of the
192 charged residue (glutamic acid) is expected to
193 compromise the solvation of E22Q peptide in water,
194 which in turn leads to a reduction of the free energy
195 barrier for fibril formation. It is also conceivable that the
196 charged state of glutamic acid introduces destabilizing
197 electrostatic interactions in the fibril itself. Therefore,
198 the substitution E \rightarrow Q may decrease the free energy
199 barrier for forming assembly-competent structures.

200 The lack of correlation between the monomeric
201 preferences of A β peptides and their observed
202 propensities to form amyloid finds support in recent
203 experimental studies. Wuthrich and co-workers [42^{*}]
204 investigated the conformational characteristics of
205 A β ₁₋₄₀^{ox} and A β ₁₋₄₂^{ox} (ox means that methionine at
206 position 35 occurs as sulfoxide) using solution NMR
207 spectroscopy and found that there is close similarity
208 between the solution structures of these peptides. The
209 only discernible difference is found in the C-terminal
210 region, starting with position 32. This is not surprising
211 given that there are two additional (isoleucine and
212 alanine) hydrophobic residues in the A β ₁₋₄₂^{ox} peptide.

213 This finding is important, because A β ₁₋₄₂ is known to
214 fibrillize faster than A β ₁₋₄₀ [43]. The study of Wuthrich
215 and co-workers suggests that the two C-terminal

216 hydrophobic residues in $A\beta_{1-42}$ should critically affect
217 the intermediate structures (oligomers) in fibril
218 formation by lowering the free energy barrier for
219 aggregation. It is also interesting that, similar to $A\beta_{10-35}$
220 [44], the structures of $A\beta_{1-40}^{ox}$ and $A\beta_{1-42}^{ox}$ peptides in
221 aqueous solution have little long-range order or easily
222 identifiable elements of secondary structure [42]. The
223 most rigid element of their structure seems to be the
224 central hydrophobic cluster (17–21), which adopts
225 similar conformations in both $A\beta_{1-40}^{ox}$ and $A\beta_{1-42}^{ox}$
226 peptides, as well as in $A\beta_{10-35}$ peptide. Thus,
227 interpeptide interactions must be taken into account to
228 understand the observed differences in the rate of
229 amyloid formation between $A\beta_{1-40}$ and $A\beta_{1-42}$.

230 Recently, two 10 ns trajectories generated by MD
231 simulations of PrP^c (Figure 1a) have been used to probe
232 the initial events in the conformational transition to the
233 aberrant aggregation-prone form [45]. It is known that
234 this transition can be driven by lowering the pH (i.e.
235 under acidic conditions) [46,47]. At neutral pH, the
236 ordered regions of PrP^c remain stable during the
237 simulation time. However, at low pH, substantial
238 conformational fluctuations in residues 109–175, which
239 include disordered N-terminal helix 1 and the two small
240 β strands (Figure 1a), are observed. The authors
241 conclude from examining several conformational
242 snapshots that there might be a tendency for strand
243 formation in helix 1. Moreover, the strands in PrP^c have
244 a tendency to lengthen. These simulations suggest that
245 a glimpse into the early events of the fibrillization
246 kinetics may be obtained using MD simulations over a
247 range of external conditions. Bioinformatic analysis
248 [31^{**},32^{**}] and recent experiments [48^{**}] suggest that
249 parts of helices 2 and 3 may also be implicated in the
250 transition from PrP^c to the scrapie form (PrP^{Sc} see
251 below).

252 **Negative design: gatekeeper residues** 253 **prevent aggregation**

254 In the cell, a large fraction of proteins with varying
255 architecture fold spontaneously by avoiding off-pathway
256 processes that lead to aggregation. To prevent aberrant
257 protein aggregation, nature employs molecular
258 chaperones — nanomachines that actively assist the
259 folding of proteins. A plausible link between the
260 underexpression of molecular chaperones and the onset
261 of certain classes of diseases suggests that these
262 nanomachines may be utilized more widely than has
263 been appreciated so far. However, it has been estimated
264 that, in *Escherichia coli*, only about 5–10% of all proteins
265 can afford to employ molecular chaperones to enable
266 them to reach the folded state [49]. Thus, as envisioned
267 by Anfinsen [50], most proteins must fold
268 spontaneously and efficiently into the native state.

269 Anfinsen's hypothesis has led to the quest to
270 understand how a polypeptide chain navigates the
271 rough energy landscape to reach the native state. The

272 past decade has seen numerous theoretical and
273 experimental advances in our understanding of how a
274 monomeric protein folds. However, from the
275 perspective of aggregation, it is crucial to understand
276 how proteins, under physiological conditions, avoid
277 aggregation. A suggestion is that spontaneously folding
278 proteins may have utilized negative design in
279 generating sequences that not only can reach the final
280 desired structure efficiently but also can avoid
281 unproductive pathways [33^{**}]. An important question
282 that arises in the context of aggregation is: are there
283 residues (gatekeepers in the terminology of Otzen and
284 Oliveberg [51]) that implement the 'negative design'
285 principle? Otzen *et al.* [52^{**}] have suggested, based on
286 re-engineering the β strand in ribosomal S6 protein
287 from *Thermus thermophilus* (Figure 2) to have a sequence
288 composition similar to that of $A\beta$ peptide, that the
289 gatekeepers, which preserve the structural integrity of
290 the wild-type protein, are charged residues. They
291 modified the $\beta 2$ strand in S6 by replacing charged
292 residues with hydrophobic residues. The resulting S6-
293 Alz mutant, in which the six charged residues are
294 replaced by hydrophobic species, forms a tetramer.
295 Based on this finding, they proposed that the charged
296 gatekeeper residues, which are not implicated in
297 monomer folding, block aggregation by an electrostatic
298 mechanism. The formation of the interfaces needed for
299 oligomerization is prevented in wild-type S6 by
300 electrostatic repulsion, but is promoted in S6-Alz by
301 favorable interactions between hydrophobic residues.

302 A systematic bioinformatic approach has recently been
303 used to identify potential gatekeeper residues in β
304 strands [33^{**}]. Motivated in part by the question posed
305 above and by the finding that the majority of *de novo*
306 designed all- β -sheet proteins tend to oligomerize,
307 Richardson and Richardson (R²) [33^{**}] have proposed a
308 set of rules for identifying aggregation-blocking
309 mechanisms in β -sheet proteins. They note that, unless
310 the edge strands utilize 'negative design', edge-to-edge
311 aggregation can easily occur in all- β -sheet proteins. To
312 understand how natural proteins avoid this
313 unproductive route, they carried out an analysis of the
314 architecture and sequence of the edge strands of β -
315 sheet proteins. Their study reveals that there are two
316 global 'blocking' strategies that nature utilizes to
317 prevent edge-to-edge aggregation.

318 **Minimization and/or protection of dangling** 319 **hydrogen bonds**

320 One of the principles that emerges from the R²
321 arguments [33^{**}] is that, in the folded states of naturally
322 occurring proteins, the number of dangling hydrogen
323 bonds (HBs) is minimized. Conversely, the presence of
324 a large number of dangling HBs promotes
325 intermolecular association. The universal interaction
326 that stabilizes β -sheet proteins is the formation of HBs.
327 Proteins with β -barrel architecture have very few
328 unsatisfied HBs. As a result, there are literally no edges
329 in their structures. In β helices, which have been

330 suggested to be the nearly ‘universal’ structure of
331 amyloid fibrils [53^{**}], the edges are protected by large
332 loops. Other β -sheet architectures, such as β propellers
333 and single β -sheet proteins, use a combination of β
334 bulges and charges to avoid aggregation.

335 A corollary of the R^2 findings is that low-stability β
336 strands with a large number of unsatisfied HBs may be
337 susceptible to aggregation. In PrP^c, it is likely that
338 frustrated helices 2 and 3 could, upon conformational
339 change, have strand conformation (see below). The
340 percentages of unsatisfied HBs are 14, 14 and 9 in
341 mouse PrP^c, Syrian hamster PrP^c and h1PrP^c,
342 respectively [32^{**}]. These are larger than the average
343 fraction (6% [54]) of residues in normal proteins that
344 have unsatisfied buried HB donors/acceptors. The
345 extended structure of helices 2 and 3 in PrP^c, together
346 with the large number of unsatisfied HBs, makes this
347 region susceptible to edge-to-edge aggregation.

348 **Inward-pointing charged residues block aggregation**

349 In the context of amyloid fibrils, β -sandwich and single
350 β -sheet proteins are of particular interest. This is
351 because disease-related proteins usually polymerize
352 (see, however, [55^{**}]) upon fibril formation into β -
353 sandwich structures [2]. Edge-to-edge aggregation in
354 naturally occurring β -sandwich proteins is prevented by
355 placing an ‘inward-pointing’ charged residue on the
356 hydrophobic side of a β strand [33^{**}]. For a pair of
357 β strands, a charged sidechain is ‘inward pointing’ if its
358 C_{α} - C_{β} vector points towards the other strand backbone.
359 Placement of just one such residue in the edge strand
360 results in a minimal change in the stability of a protein,
361 but prevents aggregation. The placement of a charged
362 residue prevents aggregation either because of
363 interstrand electrostatic repulsion, as envisioned by
364 Otzen *et al.* [52^{**}], or by the need to expose the charged
365 residues to solvent. In the latter case, the distance
366 between the β strands would be large enough to
367 prevent the formation of HBs. Thus, any charged
368 residue (+ or -) can be inward pointing provided the
369 sidechain is long enough. We will refer to the principle
370 underlying this blocking strategy as the OR² (Oliveberg-
371 Richardson-Richardson) rule.

372 The other strategy, which is not as relevant to
373 aggregation, involves creating a local β bulge, which
374 effectively disrupts HBs between β strands [33^{**}].
375 There is no sequence conservation at gatekeeper
376 positions as might be deemed necessary for monomeric
377 folding. The irregularities found in edge strands due to
378 the placement of ‘unusual’ residues are purely for the
379 purpose of negative design [33^{**}].

380 There are a few experimental amyloidogenesis studies
381 that illustrate the OR² criterion for preventing
382 aggregation.

383 *S6 and variants*

384 Otzen *et al.* [52^{**}] probed fibril formation in three 14-
385 mer peptides corresponding to residues 36–49 in the β 2
386 strand of S6. The wild-type RVEKVEELGLRRLA

387 peptide, which has a net positive charge, has seven
388 charged residues. Both wild-type peptide and the
389 double mutant E41A/E42A are soluble. Otzen *et al.*
390 noted that E41A/E42A forms amorphous (gel-like)
391 aggregates at high peptide concentration. This
392 observation points to the need for exploring phase
393 diagrams of proteins with the protein concentration and
394 other external conditions as appropriate variables [56^{**}].

395 At a relatively low protein concentration, the mutant
396 peptide S6-Alz (RVEKVAAILGLMVL A) forms insoluble
397 fibrils with morphology similar to that of A β aggregates.
398 The S6-Alz peptide, which has β -sheet structure in
399 water, has no charged residues in the middle. Because
400 the aggregation-blocking mechanism is disabled, the
401 OR² rule implies that S6-Alz would form β sandwiches
402 stabilized by interpeptide interactions between
403 hydrophobic sidechains. The middle of S6-Alz has the
404 membrane protein motif HHHHGHHHHH (H stands
405 for hydrophobic residue), which occurs with negligible
406 probability in globular proteins.

407 The OR² rule can also be used in interpreting the
408 tetramerization of the S6-Alz mutant. At high
409 concentration, S6-Alz forms tetramers, in which edge
410 strand β 2 serves as an interface. Residues 38–44 in
411 strand β 2 of one of the molecules form an antiparallel β
412 sheet with the same residues from an another molecule.
413 Similarly, residues 47–50 of β 2 form an intermolecular
414 antiparallel β sheet with the β strand (residues 89–92)
415 from another molecule. Aggregation of S6-Alz into
416 tetramers becomes possible due to double mutations
417 E41A/E42A and R46M/R47M, which remove charged
418 residues from strand β 2. This experimental result may
419 be rationalized in light of the OR² rule. The negatively
420 charged sidechains of glutamic acid residues, which
421 appear in tandem at positions 41 and 42, are placed on
422 both sides of β 2 (Figure 2). Their sidechains are
423 exposed to solvent (the relative, that is, with respect to
424 a Gly-X-Gly construct, accessible surface areas [ASAs]
425 are 0.46 and 0.44, respectively). The positively charged
426 sidechains of the two arginine residues, which occur in
427 tandem at positions 46 and 47, are also placed on
428 opposite sides of the β strand (Figure 2). Furthermore, a
429 twist in the β strand is observed next to R46 and R47.
430 According to the R^2 rule [33^{**}], these are the typical
431 mechanisms that prevent edge-to-edge aggregation in
432 single β -sheet proteins, such as S6.

433 The blocking method found in wild-type S6 is by no
434 means unique. Similar aggregation-preventing
435 mechanisms are observed in several other single β -sheet
436 proteins. For example, the edge β -strand 4 of profilin
437 (PDB code 1pne) contains two sequential charged
438 residues, R74 and D75, whose ASAs are 0.59 and 0.26,
439 respectively. In addition, several noticeable twists are
440 observed in this edge β strand, in particular, near the
441 positively charged K69. The same mechanisms seem to
442 be operative in preventing aggregation in the edge β -
443 strand 5 of chain A of monellin (PDB code 1mol). Two
444 sequential charged residues (R82 and K83, with ASAs

445 of 0.32 and 0.61, respectively) are found at the
446 beginning of this β strand. Thus, the mechanisms
447 blocking aggregation in wild-type S6 fall in the
448 categories described by R^2 [33^{**}]. As observed by Otzen
449 *et al.* [52^{**}], mutating these naturally evolved structural
450 gatekeepers in S6 should lead to tetramerization.

451 A direct test of the OR^2 rule for preventing aggregation
452 was provided by Wang and Hecht [57^{**}].
453 Combinatorially *de novo* designed β -sheet proteins built
454 of seven-residue β strands with an alternating
455 hydrophobic/polar (PHPHPH) pattern form fibrils with
456 amyloid-like characteristics. The OR^2 rule would
457 suggest that, if the middle hydrophobic residue in the
458 edge strand is replaced with lysine (i.e. PHPKPHP),
459 then the protein would be soluble. If such proteins form
460 fibrils, electrostatic repulsion or/and burial of
461 uncompensated charge would render the fibrils
462 unstable. In accord with the OR^2 rule, Wang and Hecht
463 showed that the redesigned proteins with lysine in the
464 middle of an otherwise alternating hydrophobic/polar
465 edge strand sequence do not aggregate and form
466 monomeric β -sheet structures.

467 *Fibrillization of transthyretin*

468 When TTR is subject to denaturation stress,
469 conformational fluctuations in the monomer produce a
470 state that can form amyloid fibrils [13]. The aberrant
471 aggregation of TTR is associated with spontaneous and
472 familial diseases in humans. By following the electron
473 paramagnetic resonance (EPR) spectra before and after
474 fibril formation, Serag *et al.* [58^{**}] have established the
475 arrangement of the strands in the amyloid fibrils. TTR,
476 predominantly a β -sheet protein, forms a tetramer by
477 burying hydrophobic strand H (Figure 3) at the
478 interface between the four identical monomeric units.
479 Kelly and co-workers [36^{**}] have demonstrated that
480 fluctuations (induced in denaturing environments)
481 populate a partially unfolded intermediate that is
482 susceptible to fibrillization by a nucleation and growth
483 process. Recent studies from the Yeates laboratory [58^{**}]
484 suggest that, in this state, the F, F', B and B' β strands
485 become exposed. The resulting structure can assemble
486 and propagate by head-to-head and tail-to-tail
487 arrangements, giving rise to the polymeric construct
488 $(BEFF'E'B')_n$. In this proposed arrangement, the
489 native-like interface contacts between the F and F' β
490 strands are preserved (Figure 3).

491 It was noted by Yeates and co-workers [58^{**}] that the
492 proposed architecture of TTR fibrils is consistent with
493 the Richardson studies. Here, we describe an analysis of
494 the structural characteristics of the TTR dimer (PDB
495 code 2pab), which provides additional support to the
496 proposed architecture of wild-type TTR fibrils (Figure
497 3). If the dimer is dissected into its constituents, the
498 highly hydrophobic strand H, with the largest ASA (in
499 the monomer state), is the edge strand. The R^2
500 observation would suggest that this vulnerable strand
501 will form a β sheet with other strands, which explains
502 why TTR is a tetramer in the natural state. A similar

503 analysis of the dimer suggests that the ASA of strand H
504 is greater than that of strand B, making the former more
505 susceptible to conformational fluctuations.
506 Furthermore, examination of the dimer structure
507 indicates that HH' interactions constitute the most
508 stable region in the monomer interface, which is
509 unlikely to dissolve given that the FF' interactions are
510 retained in the fibril [58^{**}]. The resulting amyloid fibrils
511 would form an additional $(AGHH'G'A')_n$ construct, a
512 possibility that was not ruled out by Yeates and co-
513 workers [58^{**}].

514 We have calculated, using the protocol described
515 elsewhere [59], the energies required to expose strands
516 B and H. The energy loss in forming the misfolded
517 structure that enables the formation of the BB' interface
518 is considerably smaller than that associated with the
519 disruption of the HH' interface. Exposure of strand B
520 requires the removal of edge strands C and D (Figure
521 3). On the other hand, exposure of strand H requires
522 breaking the entire interface (HH' and FF'), which is
523 stabilized by several sidechain contacts and HBs. The
524 bulk of the interfacial energy gain in the wild-type
525 TTR arises from the strong interactions between H and
526 H'. As a result, it is unlikely that the partially folded
527 structure involves conformational changes in the
528 interfacial region. The current computations show that
529 the use of the R^2 observation, together with the stability
530 arguments, helps us understand the architecture of
531 TTR amyloid fibrils. Because of the presence of the
532 consecutive like charges (arginine and lysine) towards
533 the end of strand B in an otherwise hydrophobic
534 environment, it is easy to predict that B and B' should
535 be arranged in an antiparallel fashion [58^{**}].

536 Another line of evidence that implicates strand B is the
537 observation that many disease-causing mutations are
538 clustered in this region. Therefore, this region of the
539 protein may be intrinsically susceptible to fluctuations
540 under suitable denaturation stress. It also follows from
541 our analysis that mutations that destabilize the interface
542 might lead to fibrils with a different architecture. The
543 converse of this has been demonstrated by Kelly and
544 co-workers [36^{**}]. They showed that the mutation
545 T119A, which stabilizes the tetramers, essentially
546 prevents fibrillization.

547 **'Frustrated' secondary structural elements** 548 **may be harbingers of a tendency to** 549 **polymerize**

550 The ease of aggregation and the morphology of the
551 aggregates depend not only on protein concentration
552 but also on other external conditions, such as
553 temperature, pH and salt concentration. Although most
554 proteins can, under suitable conditions, aggregate, the
555 observation that several disease-causing proteins form
556 amyloid fibrils under physiologically relevant conditions
557 raises the question: is aggregation or the need to avoid
558 unproductive pathways encoded in the primary
559 sequence itself? It is clear that sequences that contain a
560 patch of hydrophobic residues are prone to forming

561 aggregates [60]. However, it is known that contiguous
562 patches (three or more hydrophobic residues) occur
563 with low probability in globular proteins [61]. For
564 example, sequences with five hydrophobic residues
565 (LVFFA in A β peptide) in a row are not well
566 represented. Similarly, it is unusual to find hydrophobic
567 residues concentrated in a specific region of helices,
568 such as in helix 2 of PrP^c [32^{**}]. *De novo* design of α
569 helices or β strands based on periodic binary patterned
570 (sequences formed from hydrophobic and polar residues
571 only) sequences often forms insoluble oligomers [60].
572 The morphology of these oligomers apparently has the
573 characteristics of amyloid fibrils. These examples
574 suggest that sequence alone in some cases might reveal
575 the tendency towards aggregation of proteins.

576 It is natural to wonder if secondary structure elements
577 (SSEs) bear signatures that could reveal amyloidogenic
578 tendencies. The incompatibility of the nature of an SSE
579 in the context of the entire protein may give insights
580 into regions of the protein that may be susceptible to
581 conformational fluctuations. Two studies have proposed
582 that the extent of 'frustration' in SSEs may be a
583 harbinger of amyloid fibril formation [31^{**},32^{**}]. Because
584 reliable secondary structure prediction requires
585 knowing the context-dependent propensities and
586 multiple sequence alignments (as used in PHD, a
587 profile network from Heidelberg [62]), it is likely that
588 assessment of the extent of frustration in SSEs, rather
589 than analysis of sequence patterns, is a better predictor
590 of fibril formation. Frustration in SSEs is defined as the
591 incompatibility of the predicted (from PHD, for
592 example) secondary structure and the experimentally
593 determined structure [31^{**}]. For example, if a secondary
594 structure is predicted with high confidence to be in a β
595 strand and if that segment is found (by NMR or X-ray
596 crystallography) to be in a helix, then the structure is
597 'frustrated' (or discordant or mismatched). The α/β
598 discordance, which can be correlated with amyloid
599 formation, can be assessed using the score

$$600 S_{\alpha/\beta} = \frac{1}{L} \sum_{i=1}^L (R_i - 5), \text{ where } R_i \text{ is the reliability score}$$

601 predicted by PHD at position i of the query sequence, 5
602 is the mean score and L is the sequence length. The
603 bounds on $S_{\alpha/\beta}$ are $0 \leq S_{\alpha/\beta} \leq 4$, with maximal frustration
604 corresponding to $S_{\alpha/\beta} = 4$. Similarly, the measure $S_{\beta/\alpha}$
605 gives the extent of frustration in a region that is
606 predicted to be helical and is found experimentally to
607 be a strand. Using $S_{\alpha/\beta}$ and other structural
608 characteristics, one can make predictions of the
609 plausible regions that are most susceptible to large
610 conformational fluctuations.

611 PrP^c and Dpl

612 Using the above concept of SSE frustration, the 23-
613 residue sequence
614 QNRFVHDCVNITIKQHTVTTT^TTK in mouse PrP^c
615 (Figure 1a), with a score of 1.83, was assessed to be
616 frustrated or discordant [32^{**}]. Other measures of
617 quantifying the structure showed that the maximal

618 frustration is localized in the second half (C-terminal of
619 helix 2) [32^{**}]. The validity of this prediction finds
620 support in the analysis of mutants of the PRNP gene
621 associated with inherited transmissible spongiform
622 encephalopathies (familial Creutzfeldt-Jakob disease
623 [CJD] and fatal familial insomnia [FFI]). According to
624 SWISS-PROT [63], seven disease-causing point
625 mutations (D178N, V180I, T183A, H187R, T188R,
626 T188K and T188A) are localized in helix 2. (We have
627 used the sequence numbering for mouse PrP^c). A naive
628 use of propensities to form helices (similar to those of
629 Chou and Fasman [64]) would suggest that, with the
630 exception of D178N, all other point mutations should
631 lead to better helix formation. However, the $S_{\alpha/\beta}$ scores
632 for the mutants are 1.94, 1.80, 1.30, 1.80, 1.54, 1.94 and
633 1.94 for D178N, V180I, T183A, H187R, T188K, T188R
634 and T188A respectively. Thus, in all these mutants,
635 helix 2 is frustrated, making it susceptible to the
636 conformational fluctuations that have to occur before
637 fibrillization. The differences in $S_{\alpha/\beta}$, which can be
638 correlated with local stability, suggest that stability
639 alone may not be a good indicator of the kinetics of
640 amyloid formation.

641 As stated earlier, there are many unsatisfied HBs in
642 PrP^c. Several of these mismatches are found in helices 2
643 and 3 (Figure 1a). If these regions become exposed
644 upon PrP^c→PrP^{c*} transition, then minimization of the
645 dangling HBs can be accomplished by polymerization
646 of PrP^{c*}. Measures of frustration and other structural
647 characteristics suggest that even segments of the rigid
648 and ordered part of PrP^c may play a key role in the
649 production of PrP^{c*}. When the theoretical studies
650 (which showed that regions of helices 2 and 3 could be
651 involved in the PrP^c→PrP^{c*} transition) appeared, there
652 was no direct experimental support. Subsequently,
653 using ¹⁵N-¹H two-dimensional NMR measurements as a
654 function of pressure, Kuwata *et al.* [48^{**}] have concluded
655 that, in PrP^{c*}, helices 2 and 3 are disordered. The
656 disordered metastable intermediates may be precursors
657 in the templated assembly that converts PrP^c to PrP^{c*}.
658 This study shows, in accord with the theoretical
659 predictions [31^{**},32^{**}], that the core of PrP^c is involved
660 in producing the assembly-competent PrP^{c*}. Although
661 the mechanism leading to PrP^{sc} is still unknown, it is
662 worth emphasizing that the concept of SSE frustration
663 in the wild-type proteins may be a useful indicator of
664 the regions that harbor amyloidogenic tendencies.

665 The gene encoding the Doppel protein (Dpl), termed
666 *Prnd* [65], is a paralog of the prion protein gene, *Prnp*, to
667 which it has about 25% identity. Normally, Dpl is not
668 expressed in the central nervous system, but it is up-
669 regulated in mice with knockout *Prnp* gene. In such
670 cases, overexpression of Dpl causes ataxia with Purkinje
671 cell degeneration [65], which in turn can be cured by
672 the introduction of one copy of the wild-type PrP
673 mouse gene [66]. NMR studies of the three-
674 dimensional structure of mouse Dpl [67] (Figure 1b)
675 showed that it is structurally similar to PrP^c. However,

676 PrP^c and Dpl produce diseases of the central nervous
677 system using very different mechanisms: PrP^c causes
678 disease only after conversion to the PrP^{Sc} form, whereas
679 simple overexpression of Dpl, with no requirement for
680 the scrapie form, causes ataxia. The markedly different
681 disease mechanisms of PrP and Dpl would suggest, in
682 light of the findings for PrP^c, that mouse Dpl (PDB
683 code 1i17) would not be frustrated. Indeed, prediction
684 of secondary structure by PHD [62] for mouse Dpl
685 correlates well with the experimentally derived
686 structure. The only difference between the predicted
687 and derived structures of Dpl is found in the first β -
688 strand region, which is predicted to be helical by PHD.
689 However, corresponding $S_{\beta,\alpha}$ is -3.0 , indicating that this
690 α -helix prediction is unreliable as this sequence has low
691 complexity. Also, analysis of mouse Dpl with the
692 WHAT CHECK program [68] reveals that, on average,
693 there are only eight unsatisfied buried HB
694 donors/acceptors, representing 7.4% of all residues in
695 mouse Dpl. This is comparable with the average value
696 of 6% found in normal proteins, but it is markedly
697 smaller than the 14% seen in mouse PrP (PDB code
698 1ag2). This analysis rationalizes the lack of observed
699 scrapie formation in Dpl.

700 **Structures of amyloid fibrils**

701 To understand the assembly mechanisms of amyloid
702 fibrils, it is necessary to determine the fibril structures
703 in atomic detail. Noncrystallinity and insolubility of the
704 amyloid fibrils have made it difficult to obtain high-
705 resolution fibril structures. Nevertheless, in the past
706 few years, a variety of experimental and computational
707 techniques have been used to provide a glimpse into
708 the detailed architecture of fibrils in a variety of
709 systems. Here, we focus on three such systems.

710 **Human prion protein dimer**

711 In an important paper, Knaus *et al.* [69**] announced a 2
712 Å crystal structure of the dimeric form of the human
713 prion protein (residues 90–231). The structure suggests
714 that dimerization occurs by a domain-swap mechanism,
715 in which helix 3 from one monomer packs against helix
716 2 from another. In fact, Eisenberg and co-workers [70]
717 have suggested that a domain-swapping mechanism
718 may be a general route for amyloid fibril formation. The
719 electron density map seems to suggest structural
720 fluctuations in residues 189–198, which coincide with
721 the maximally frustrated region predicted theoretically
722 [31**,32**]. The dimer interface is stabilized by residues
723 that are in helix 2 in the monomeric NMR structure.
724 The header of the PDB file of the monomeric structure
725 of human PrP^c indicates that helix 2 ends at residue 194
726 and helix 3 begins at 200. The domain-swapped dimer
727 structure shows that residues 190–198 exist largely in a
728 β -strand conformation. It appears that the $\alpha \rightarrow \beta$
729 transition minimizes frustration. One implication of the
730 dimer structure is that oligomerization occurs by
731 domain swapping, which, in PrP^c, may also involve the
732 disulfide bond between the cysteine residues at 179 and

733 214. The role of the disulfide bond in PrP^{Sc} formation
734 remains controversial.

735 **Structural characteristics of A β fibrils**

736 Recent solid-state NMR studies have provided, for the
737 first time, direct measurements of interatomic distances
738 between labeled residues in A β amyloid fibrils [22].
739 These studies have suggested that the arrangements of
740 the strands in the fibrils depend on the length of the
741 peptide. The parallel in-register organization of
742 peptides in β sheets was proposed for both A β_{10-35} [21**]
743 and A β_{1-40} [23*,71**] fibrils. Such an organization raises
744 the question: how is the destabilizing electrostatic
745 repulsion due to close placement of like charges in
746 parallel registry accommodated in A β_{1-40} fibrils? To
747 answer this question, Tycko and co-workers [71**]
748 proposed a novel structural model for A β_{1-40} peptide
749 organization into fibrils. The measurement of
750 correlations between ¹³C and ¹⁵N chemical shifts to
751 probe the conformations (in terms of ϕ and ψ angles) of
752 individual residues in A β_{1-40} peptides showed that
753 residues 12–24 and 30–40 adopt β -strand structure.
754 Residues 25–29 form a bend. On the basis of these and
755 previous findings [22,23*], Tycko and co-workers
756 proposed that there are two β strands in A β_{1-40} , which
757 form an in-register parallel β sheet. The β sheet HBs
758 run parallel to the fibril axis. The formation of an
759 intrapeptide salt bridge between charged residues D23
760 and K28 lends stability to the interstrand interactions.
761 Taking into account the measurements of mass-per-
762 length by scanning transmission electron spectroscopy,
763 they proposed that individual A β_{1-40} peptides are
764 juxtaposed to form a dimer, which serves as an
765 elementary building block of parallel β sheets. Their
766 structural model is based on the premise, which finds
767 support in MD simulations of A β_{16-22} peptides [30**],
768 that fibril structures form by maximizing favorable
769 hydrophobic and electrostatic (salt bridge) interactions.

770 The structural model for A β_{1-40} amyloids proposed by
771 Tycko and co-workers was independently predicted by
772 Ma and Nussinov [27*]. Using MD simulations, they
773 probed the stabilities of various structural arrangements
774 of A β_{10-35} peptides. Although the simulation results
775 cannot be conclusive because of the short duration and
776 the lack of equilibration of the initial structures, they
777 provide valuable insights into the fibrillar architecture.
778 Similar to the model of Tycko and co-workers, a turn (at
779 positions 24–27) is proposed, which is reinforced by the
780 intrapeptide salt bridge D23–K28.

781 In contrast to A β_{1-40} , a different structural organization is
782 envisioned for A β_{10-35} fibrils. To maximize hydrophobic
783 interactions, two A β_{10-35} peptides in turn conformations
784 are docked end-to-end, locking unmatched residues 10–
785 16. A hydrophobic core is centered near position L34.
786 Thus, both solid-state NMR measurements and MD
787 simulations suggest that the parallel in-registry structure
788 of A β peptides with a turn in the middle appears to be
789 the most stable arrangement for long A β peptides. The
790 proposed structure for A β_{10-35} fibrils [27*] is at variance

791 with the structure suggested by Lynn and co-workers
792 [21⁷²]. In contrast to A β ₁₋₄₀ [71⁷²] and A β ₁₀₋₃₅ [21⁷²], the
793 16-22 and 34-42 fragments have been shown to form
794 antiparallel β sheets [20,73]. We found that A β ₁₆₋₂₂ forms
795 an in-registry antiparallel organization, which is favored
796 by interpeptide K16-D22 salt bridges and hydrophobic
797 interactions between aromatic residues [30⁷²].

798 Experiments so far have not probed the structural
799 organization of short peptides in fibrils beyond single β
800 sheets. Several MD simulations have been performed to
801 examine the three-dimensional structures of amyloid
802 fibrils [27⁷⁴]. The interesting study of Ma and
803 Nussinov [27⁷⁴] found that A β ₁₆₋₂₂ forms the most stable
804 fibril structure, which is arranged in antiparallel in-
805 registry β sheets that propagate parallel to each other.
806 This structural organization provides close contacts
807 between oppositely charged lysine and glutamic acid
808 residues, and also establishes optimal (parallel) registry
809 between phenylalanine residues in neighboring β
810 sheets. Simulations of 24-mer fibril blocks revealed a
811 significant twist angle of 15° per peptide.

812 Structure of aggregates of tau protein

813 Paired helical filaments (PHFs), which are primarily
814 aggregates of the microtubule-associated tau protein,
815 also accumulate in neurons of patients with Alzheimer's
816 disease. The prevailing view is that the insoluble
817 filaments are composed of β sheets, giving credence to
818 the notion that the formation of such structures is a
819 universal characteristic of all disease-causing proteins.
820 The soluble tau protein, in the monomeric form, is
821 known to be unstructured [75]. Using far-UV circular
822 dichroism (CD) and Fourier transform infrared (FTIR)
823 spectroscopy, Sadqi *et al.* [55⁷⁶] showed that the PHF,
824 contrary to popular belief, is predominantly helical. In
825 this case, there must be a structural transition in the
826 major protein component of PHF, namely tau, from a
827 random coil to α helix [55⁷⁶].

828 Multiple routes to fibril formation

829 Although significant progress has been made in the
830 determination of low-resolution structures of fibrils,
831 relatively little is known, at the molecular level, about
832 the cascade of events that leads to aggregation. Several
833 experimental studies suggest that, generically, fibril
834 formation exhibits all the characteristics of a nucleation-
835 growth process [16]. The kinetics of fibril formation has
836 a lag phase provided the protein concentration exceeds
837 a critical value. The lag phase disappears if a seed or
838 preformed nucleus is present in the supersaturated
839 solution. The seeded growth of fibrils, which closely
840 resembles the templated assembly envisioned by
841 Griffith to explain self-replication of proteins [77], has
842 been explicitly verified in simple lattice models
843 [56⁷⁸].

844 One of the most popular beliefs is that fibrillization
845 requires partial unfolding of the native state or partial
846 folding of the unfolded state [10,12-14]. Both events,
847 which are likely to involve crossing free energy barriers
848 (Figure 4), produce the assembly-competent structure

849 N*. The N* state in TTR, which has a higher free
850 energy than the native state N, is formed upon the
851 unraveling of edge strands C and D, thus exposing
852 strand B [13,58⁷²]. One can also envision a scenario in
853 which N* has a lower free energy than N, thus making
854 the monomeric native state metastable (Figure 4). We
855 conjecture that amyloidogenic proteins, in which nearly
856 complete transformation of the structure takes place
857 upon fibrillization, may follow the second scenario.
858 Both of these possibilities follow from an energy
859 landscape perspective of aggregation [79⁷²]. In both
860 cases (Figure 4), fibrillization kinetics should be
861 determined by an 'unfolding' free energy barrier
862 separating the N and N* states. Recent studies of the
863 fibrillization of PrP^c and TTR provide experimental
864 support for this concept [36⁷²]. The perspective
865 sketched in Figure 4 also suggests that the free energy
866 of stability of N may not be a good indicator of the rates
867 of fibrillization.

868 In scenario I, the amyloidogenic state N* is formed by
869 denaturation stress. The production of N* in scenario II
870 can occur by two distinct routes. If N is metastable, as is
871 apparently the case for PrP^c [80⁷²], then conformational
872 fluctuations can lead to N*. Alternatively, formation of
873 N* can also be triggered by intermolecular interactions
874 (this possibility presumably applies for A β peptides). In
875 the latter case, N* can only form when the protein
876 concentration exceeds a threshold value.

877 To better understand the kinetics of fibrillization, it is
878 necessary to characterize the early events and pathways
879 leading to the formation of the critical nucleus. In terms
880 of the two scenarios outlined above, the structures of
881 N*, the ensemble of transition state structures and the
882 conformations of the critical nuclei must be known to
883 fully understand the assembly kinetics. A significant
884 step in this direction has been taken by Teplow and co-
885 workers [29⁷²], who have followed the growth of fibrils
886 for 18 peptides, including A β ₁₋₄₀ and A β ₁₋₄₂. In all cases,
887 the formation of amyloids by A β ₁₋₄₀ and A β ₁₋₄₂ is
888 preceded by the formation of the intermediate
889 oligomeric state with high α -helical content. This is
890 remarkable given that both the monomers and fibrils
891 have little or no α -helical content. Therefore, the
892 transient accumulation of α -helical structure represents
893 an obligatory (on-pathway) intermediate state, which
894 coincides with the onset of oligomerization.

895 Because it is experimentally difficult to atomically map
896 the events leading to fibrillization, we have carried out
897 multiple long MD simulations to probe the
898 oligomerization of A β ₁₆₋₂₂ peptides [30⁷²]. This peptide,
899 which is disordered in the monomeric form, assembles
900 into an antiparallel β structure through interpeptide
901 interactions. Even in the oligomerization of these small
902 peptides from the A β family, the assembly was
903 preceded by the formation of an on-pathway α -helical
904 intermediate. Based on our findings and the work by
905 Teplow and co-workers, we postulated that the

906 formation of oligomers rich in α -helical structure may
907 be a universal mechanism for A β peptides.

908 Formation of the on-pathway α -helical intermediate
909 may be rationalized using the following arguments. The
910 initial events involve the formation of 'disordered'
911 oligomers, driven by hydrophobic interactions that
912 reduce the effective volume available to each A β
913 peptide. In the confined space, peptides adopt α -helical
914 structure. Further structural changes are determined by
915 the requirement of maximizing the number of favorable
916 hydrophobic and electrostatic interactions. This can be
917 achieved if A β peptides adopt ordered extended β -like
918 conformations provided that oligomers contain a
919 sufficiently large number of peptides.

920 There is some similarity between the aggregation
921 mechanism postulated for A β peptides and the
922 nucleated conformational conversion (NCC) model
923 envisioned for the conversion of Sup35 to [PSI⁺] in
924 *Saccharomyces cerevisiae*. By studying the assembly
925 kinetics of Sup35, Serio *et al.* [81^{**}] proposed the NCC
926 model, which combines parts of the templated assembly
927 and nucleation-growth mechanisms. The hallmark of
928 the NCC model is the formation of a critical-sized
929 mobile oligomer, in which Sup35 adopts a conformation
930 that may be distinct from its monomeric random coil or
931 the conformation it adopts in the aggregated state. The
932 formation of a critical nucleus, to which other Sup35 can
933 assemble, involves a conformational change to the state
934 that it adopts in self-propagating [PSI⁺]. The α -helical
935 intermediate seen in A β peptides may well correspond
936 to the mobile oligomer that has the 'wrong'
937 conformation to induce further assembly. Thus, as
938 noted by Lindquist and co-workers [81^{**}], NCC may
939 serve as a unifying model for protein aggregation.

940 Conclusions

941 The development of methods to envision the structure
942 of amyloid fibrils has enabled us to obtain molecular
943 insights into the assembly process itself. Computational
944 and experimental studies are beginning to provide
945 detailed information, at the residue level, about the
946 regions in a given protein that harbor amyloidogenic
947 tendencies. We have harnessed these developments to
948 propose tentative ideas on the molecular basis of
949 protein aggregation. These principles (or, more
950 precisely, rules of thumb) may be useful in the
951 interpretation and design of new experiments.

952 Despite the great progress that has been made in the
953 past few years, several outstanding issues still require
954 clarification. Are there common pathways involved in
955 the self-assembly of fibrils? Because of the paucity of
956 the structural description of the intermediates involved
957 in the aggregation process, a definitive answer cannot
958 be currently provided. The energy landscape
959 perspective, summarized briefly in Figure 4, suggests
960 that multiple scenarios for assembly exist. Although the
961 generic nucleation-growth mechanism governs fibril
962 formation, the details can vary considerably. A complete
963 understanding will require experiments along the lines

964 initiated by Teplow and co-workers [29^{**}]. The
965 microscopic basis for the formation of distinct strains in
966 mammalian prions and in yeast prions remains a
967 mystery. Are these merely associated with the
968 heterogeneous seeds or are there unidentified
969 mechanisms that lead to their formation? What are the
970 factors that determine the variations in the fibrillization
971 kinetics for the wild type and the mutants? A tentative
972 proposal is that the kinetics of polymerization is
973 determined by the rate of production of N^{*} (Figure 4)
974 [82], which in turn is controlled by barriers separating N
975 and N^{*} [32^{**},36^{**}]. In this scenario, the stability of N
976 plays a secondary role. The generality of this
977 observation has not yet been established. Finally, how
978 can one design better therapeutic agents based on
979 enhanced knowledge of the assembly mechanism?
980 Even in the case of sickle cell disease, viable therapies
981 began to emerge only long after the biophysical aspects
982 of gelation were understood [83].

983 Update

984 Recently, Bitan *et al.* [86] showed that A β_{1-40} and A β_{1-42}
985 oligomerize by distinct pathways. The oligomerization
986 of this class of peptides follows scenario II in Figure 4.
987 The distinct rates of fibril formation of A β_{1-40} and A β_{1-42}
988 can be rationalized in terms of the variations in the free
989 energy barrier heights separating U and N^{*}. A
990 quantitative assessment of this proposal will require
991 temperature-dependent measurements of
992 oligomerization rates.

993 The scenarios for fibrillization shown in Figure 4 imply
994 that aggregation may be prevented by destabilizing N^{*}.
995 Hammarstrom *et al.* [87] have recently used this strategy
996 to devise a way to prevent transthyretin amyloidosis by
997 having inhibitors increase the kinetic barrier separating
998 N and N^{*}. Based on this study, they propose that using
999 the small-molecule binding strategy is an effective way
1000 of treating a number of amyloid diseases. This study
1001 also highlights the use of biophysical methods in
1002 coming up with plausible therapies for this class of
1003 amyloid disease.

1004 Acknowledgements

1005 We thank John Straub and Robert Tycko for several useful
1006 conversations. The comments by David Teplow are greatly
1007 appreciated. This work was supported in part by a grant from the
1008 National Institutes of Health (IR01 NS41356-01).

1009 References and recommended reading

1010 Papers of particular interest, published within the annual period of
1011 review, have been highlighted as:

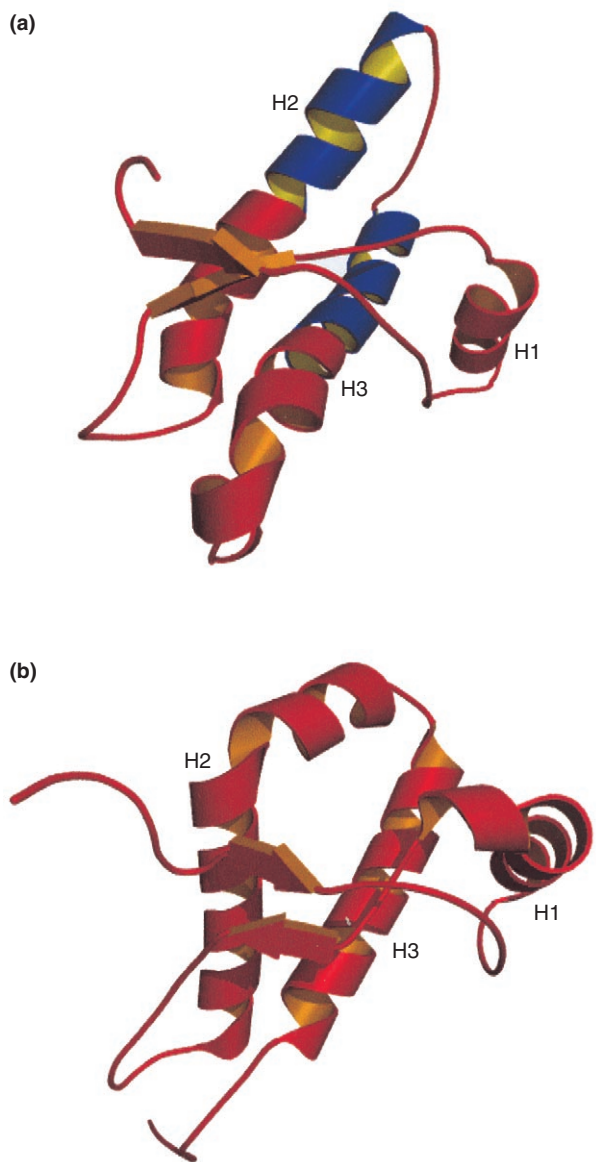
- of special interest
 - of outstanding interest
- 1014 1. Selkoe DJ: **Alzheimer's disease: genes, proteins, and**
1015 **therapy.** *Physiol Rev* 2001, **81**:741-766.
 - 1016 2. Hardy J, Selkoe DJ: **The amyloid hypothesis of Alzheimer's**
1017 **disease: progress and problems on the road to**
1018 **therapeutics.** *Science* 2002, **297**:353-356.
 - 1019 3. Prusiner S: **Prions.** *Proc Natl Acad Sci USA* 1998,
1020 **95**:12580-12585.
 - 1021 4. Scott MR, Robert W, Ironside J, Nguyen H-OB, Tremblay P,
1022 DeArmond SJ, Prusiner SB: **Compelling transgenic**
1023 **evidence for transmission of bovine spongiform**

- 1024 **encephalopathy prions to humans. *Proc Natl Acad Sci*
1025 *USA* 1999, **96**:15137-15142.**
- 1026 5. Kisilevsky R: **Review: Amyloidogenesis - unquestioned**
1027 **answers and unanswered questions. *J Struct Biol* 2000,
1028 **130**:99-108.**
- 1029 6. Lambert MP, Barlow AK, Chromy BA, Edwards C, Freed R,
1030 Liosatos M, Morgan TE, Rozovsky I, Trommer B, Viola KL:
1031 **Diffusible, nonfibrillar ligands derived from A β 1-42 are**
1032 **potent central nervous system neurotoxins. *Proc Natl*
1033 *Acad Sci USA* 1998, **95**:6448-6453.**
- 1034 7. Walsh DM, Hartley DM, Kusumoto Y, Fezoui Y, Condron MM,
1035 Lomakin A, Benedek GB, Selkoe DJ, Teplow DB: **Amyloid β -**
1036 **protein fibrillogenesis. Structure and biological activity of**
1037 **protofibrillar intermediates. *J Biol Chem* 1999,
1038 **274**:25945-25952.**
- 1039 8. Dobson CM: **Protein misfolding, evolution and disease.**
1040 *Trends Biochem Sci* 1999, **24**:329-332.
- 1041 9. Chiti F, Webster P, Taddei N, Clark A, Stefani M, Ramponi G,
1042 Dobson CM: **Designing conditions for *in vitro* formation of**
1043 **amyloid protofilaments and fibrils. *Proc Natl Acad Sci*
1044 *USA* 1999, **96**:3590-3594.**
- 1045 10. Rochet JC, Lansbury PT: **Amyloid fibrillogenesis: themes**
1046 **and variations. *Curr Opin Struct Biol* 2000, **10**:60-68.**
- 1047 ••11. Bucciantini M, Giannoni E, Chiti F, Baroni F, Formigli L,
1048 Zurdo J, Taddei N, Ramponi G, Dobson CM, Stefani M:
1049 **Inherent toxicity of aggregates implies a common**
1050 **mechanism for protein misfolding diseases. *Nature* 2002,
1051 **416**:507-511.**
- 1052 It is shown that species that form early in the aggregation of
1053 proteins (SH3 domain and bovine phosphatidyl-inositol 3' kinase)
1054 that are not associated with known diseases may be inherently
1055 cytotoxic. A clear implication of this study is that natural proteins
1056 have evolved not only to fold to the desired folded state but also to
1057 avoid aggregation.
- 1058 12. Kelly JW: **Alternative conformations of amyloidogenic**
1059 **proteins govern their behavior. *Curr Opin Struct Biol*
1060 1996, **6**:11-17.**
- 1061 13. Kelly JW: **The alternative conformations of amyloidogenic**
1062 **proteins and their multi-step assembly pathways. *Curr*
1063 *Opin Struct Biol* 1998, **8**:101-106.**
- 1064 14. Fink AL: **Protein aggregation: folding aggregates,**
1065 **inclusion bodies and amyloid. *Fold Des* 1998, **3**:R9-R23.**
- 1066 15. Eaton WA, Hofrichter J: **Sickle cell hemoglobin**
1067 **polymerization. *Adv Protein Chem* 1990, **40**:63-279.**
- 1068 16. Harper JD, Lansbury PT: **Models of amyloid seeding in**
1069 **Alzheimer's disease and scrapie: mechanistic truths and**
1070 **physiological consequences of time-dependent stability**
1071 **of amyloid proteins. *Annu Rev Biochem* 1997, **66**:385-407.**
- 1072 17. Bessen RA, Kocisko DA, Raymond GJ, Nandan S, Lansbury
1073 PT, Caughey B: **Non-genetic propagation of strain-specific**
1074 **properties of scrapie prion protein. *Nature* 1995, **375**:698-
1075 700.**
- 1076 18. Collinge J, Sidle KC, Meads J, Ironside J, Hill AF: **Molecular**
1077 **analysis of prion strain variation and the etiology of new**
1078 **variant CJD. *Nature* 1996, **383**:685-690.**
- 1079 19. Safar J, Wille H, Itri V, Groth D, Serban H, Torchia M, Cohen
1080 FE, Prusiner SB: **Eight prion strains have PrP^{Sc} molecules**
1081 **with different conformations. *Nat Med* 1998, **4**:1157-1165.**
- 1082 20. Lansbury PT, Costa PR, Griffiths JM, Simon EJ, Auger M,
1083 Halverson K, Kocisko DA, Hendsch ZS, Ashburn TT, Spencer
1084 R *et al.*: **Structural model for the beta-amyloid fibril based**
1085 **on interstrand alignment of an antiparallel-sheet**
1086 **comprising a C-terminal peptide. *Nat Struct Biol* 1995,
1087 **2**:990-998.**
- 1088 ••21. Burkoth TS, Benzinger T, Urban V, Morgan DM,
1089 Gregory DM, Thiyagarajan P, Botto RE, Meredith SC, Lynn
1090 DG: **Structure of the β -amyloid(10-35) fibril. *J Am Chem*
1091 *Soc* 2000, **122**:7883-7889.**
- 1092 The authors show that A β ₁₀₋₃₅ strands are arranged in a parallel
1093 manner in the fibrils. This study also emphasizes cooperative
1094 motion of hydrogen bonds that stabilize the parallel arrangement
1095 of the A β ₁₀₋₃₅ peptides.
- 1096 22. Tycko R: **Solid-state NMR as a probe of amyloid fibril**
1097 **structure. *Curr Opin Chem Biol* 2000, **4**:500-506.**
- 1098 •23. Antzutkin ON, Balbach JJ, Leapman RD, Rizzo NW, Reed J,
1099 Tycko R: **Multiple quantum solid-state NMR indicates a**
1100 **parallel, not antiparallel, organization of β -sheets in**
1101 **Alzheimer's β -amyloid fibrils. *Proc Natl Acad Sci USA*
1102 2000, **97**:13045-13050.**
- 1103 One of the first reports to suggest that A β ₁₋₄₀ peptides are
1104 arranged as parallel β sheets in amyloid fibrils.
- 1105 24. Harper JD, Wong SS, Lieber CM, Lansbury PT: **Assembly of**
1106 **A β amyloid protofibrils: an *in vitro* model for a possible**
1107 **early event in Alzheimer's disease. *Biochemistry* 1999,
1108 **38**:8972-8980.**
- 1109 25. Jimenez JL, Nettleton EJ, Bouchard M, Robinson CV, Dobson
1110 CM, Saibil HR: **The protofilament structure of insulin**
1111 **amyloid fibrils. *Proc Natl Acad Sci USA* 2002, **99**:9196-
1112 9201.**
- 1113 26. Serpell JC, Smith JM: **Direct visualisation of the beta-sheet**
1114 **structure of synthetic Alzheimer's amyloid. *J Mol Biol*
1115 2000, **299**:225-231.**
- 1116 •27. Ma B, Nussinov R: **Stabilities and conformations of**
1117 **Alzheimer's β -amyloid peptide oligomers (A β ₁₆₋₂₂, A β ₁₆₋₃₅⁺**
1118 **and A β ₁₀₋₃₅): sequence effects. *Proc Natl Acad Sci USA*
1119 2002, **99**:14126-14131.**
- 1120 MD simulations were used to assess the stabilities of A β peptides.
1121 By comparing the stabilities of different arrangements of peptides
1122 in the fibril, the authors have proposed a novel structural model for
1123 aggregates of A β peptides.
- 1124 28. Walsh DM, Klyubin I, Fadeeva JV, Cullen WK, Anwyl R,
1125 Wolfe MS, Rowan MJ, Selkoe DJ: **Naturally secreted**
1126 **oligomers of amyloid beta protein potently inhibit**
1127 **hippocampal long-term potentiation *in vivo*. *Nature* 2002,
1128 **416**:535-539.**
- 1129 ••29. Kirkitadze MD, Condron MM, Teplow DB: **Identification**
1130 **and characterization of key kinetic intermediates in**
1131 **amyloid β -protein fibrillogenesis. *J Mol Biol* 2001,
1132 **312**:1103-1119.**
- 1133 One of the first studies to describe the pathways in the assembly
1134 of A β peptides into fibrils. By studying the assembly kinetics of 18
1135 different A β peptides, the authors suggest that fibril formation is
1136 preceded by the transient population of on-pathway α -helical
1137 intermediates.
- 1138 ••30. Klimov DK, Thirumalai D: **Dissecting the assembly of**
1139 **A β ₁₆₋₂₂ amyloid peptides into antiparallel β -sheets.**
1140 *Structure* 2003, **11**:295-307.
- 1141 Using a series of MD simulations, it is shown that A β ₁₆₋₂₂ peptides
1142 form antiparallel β -sheet structures. Even in this system, α -helical
1143 intermediates are transiently populated. This led the authors to
1144 propose that fibril formation by A β peptides, which occurs by
1145 maximizing the number of salt bridges and hydrophobic
1146 interactions, must involve oligomers with high α -helical content.
- 1147 ••31. Kallberg Y, Gustafsson M, Persson B, Thyberg J,
1148 Johansson J: **Prediction of amyloid fibril-forming proteins.**
1149 *J Biol Chem* 2001, **276**:12945-12950.
- 1150 This study shows that several amyloid-forming proteins harbor α
1151 helices in regions that are theoretically predicted to be β strands.
1152 Using this incompatibility, the authors predicted the specific
1153 regions of PrP^c and A β peptides that may be involved in fibril
1154 formation.
- 1155 ••32. Dima RI, Thirumalai D: **Exploring the propensities of**
1156 **helices in PrP^c to form β sheet using NMR structures and**
1157 **sequence alignments. *Biophys J* 2002, **83**:1268-1280.**
- 1158 Using several sequence alignments and structural characteristics
1159 of PrP^c, including the concept of frustration of SSEs (see also

- [31**]), the authors predict that helices 2 and 3 are implicated in the conformational transition from PrP^c to PrP^{sc}.
- 1162 ••33. Richardson JS, Richardson DC: **Natural β -sheet**
1163 **proteins use negative design to avoid edge-to-edge**
1164 **aggregation.** *Proc Natl Acad Sci USA* 2002, **99**:2754-
1165 2759.
- 1166 This novel study illustrates the general strategies that naturally
1167 occurring β sheets use to avoid aggregation. The principles that
1168 emerge from this paper are not only relevant to the prediction of
1169 regions in proteins that are susceptible to aggregation, but also
1170 are important in the *de novo* design of proteins with β -sheet
1171 architecture.
- 1172 34. Esler WP, Stimson ER, Lachenmann MJ, Ghilardi JR, Lu Y,
1173 Vinters HV, Mantyh PW, Lee JP, Maggio JE: **Activation**
1174 **barriers to structural transition determine deposition**
1175 **rates of Alzheimer's disease.** *J Struct Biol* 2000, **130**:174-
1176 183.
- 1177 35. Sian AK, Frears ER, El-Agnaf OA, Patel BP, Manca MF,
1178 Siligardi G, Hussain R, Austen BM: **Oligomerization of β -**
1179 **amyloid of the Alzheimer's and the dutch-cerebral-**
1180 **haemorrhage.** *Biochem J* 2000, **349**:299-308.
- 1181 ••36. Hammarstrom P, Jiang X, Hurshman AR, Powers ET,
1182 Kelly JW: **Sequence-dependent denaturation energetics: a**
1183 **major determinant in amyloid disease diversity.** *Proc Natl*
1184 *Acad Sci USA* 2002, **99**:16427-16432.
- 1185 By studying the kinetics of polymerization of wild-type TTR and
1186 several mutants, the authors suggest that unfolding rates of the
1187 functional state of the normal protein are a key determinant of
1188 aggregation. A similar conclusion has been reached in [32**] in the
1189 context of PrP^c.
- 1190 37. Watson DJ, Landers AD, Selkoe DJ: **Heparin-binding**
1191 **properties of the amyloidogenic peptides A β and amylin.**
1192 *J Biol Chem* 1997, **272**:31617-31624.
- 1193 38. Miravalle L, Tokuda T, Chiarle R, Giaccone G, Bugiani O,
1194 Ragliavini F, Frangione B, Ghiso J: **Substitutions at codon**
1195 **22 of Alzheimer's A β peptide induce diverse**
1196 **conformational changes and apoptotic effects in human**
1197 **cerebral endothelial cells.** *J Biol Chem* 2000, **275**:27110-
1198 27116.
- 1199 39. Massi F, Peng JW, Lee JP, Straub JE: **Simulation study of**
1200 **the structure and dynamics of the Alzheimer's amyloid**
1201 **peptide congener in solution.** *Biophys J* 2001, **80**:31-44.
- 1202 40. Massi F, Straub JE: **Probing the origins of increased**
1203 **activity of the E22Q Dutch mutant of the Alzheimer's β -**
1204 **amyloid peptide.** *Biophys J* 2001, **81**:697-709.
- 1205 ••41. Massi F, Klimov D, Thirumalai D, Straub JE: **Charged**
1206 **states rather than propensity for β -structure determine**
1207 **enhanced fibrillogenesis in wild-type Alzheimer's β -**
1208 **amyloid peptide compared to E22Q Dutch mutant.** *Protein*
1209 *Sci* 2002, **11**:1639-1647.
- 1210 To test the hypothesis that differences in the tendency to form β
1211 strands may explain the variations in the deposition rates of wild-
1212 type A β and the E22Q mutant, the authors performed a series of
1213 MD simulations. They showed that the desolvation penalty, rather
1214 than intrinsic preferences for β structure, explains the differences
1215 in the fibrillization kinetics.
- 1216 ••42. Riek R, Guntert P, Dobeli H, Wipf B, Wuthrich K: **NMR**
1217 **studies in aqueous solution fail to identify significant**
1218 **conformational differences between the monomeric**
1219 **forms of two Alzheimer peptides with widely different**
1220 **plaque-competence, A β ₁₋₄₀^{ox} and A β ₁₋₄₂^{ox}.** *Eur J*
1221 *Biochem* 2001, **268**:5930-5936.
- 1222 The lack of differences in the solution NMR structures of
1223 A β ₁₋₄₀^{ox} and A β ₁₋₄₂^{ox} shows that monomer conformations alone
1224 are not indicative of the mechanism of polymerization.
- 1225 43. Jarrett JT, Berger EP, Lansbury PT: **The carboxy terminus of**
1226 **β amyloid protein in critical for the seeding of amyloid**
1227 **formation: implications for the pathogenesis of**
1228 **Alzheimer's disease.** *Biochemistry* 1993, **32**:4693-4697.
- 1229 44. Lee JP, Stimson ER, Ghilardi JR, Mantyh PW, Lu YA, Felix
1230 AM, Llanos W, Behbin A, Cummings M, Criekinge MV *et al.*:
1231 **¹H NMR of A β amyloid peptide congeners in water**
1232 **solution. Conformational changes correlate with plaque**
1233 **competence.** *Biochemistry* 1995, **34**:5191-5200.
- 1234 ••45. Alonso DOV, DeArmond SJ, Cohen FE, Daggett V: **Mapping**
1235 **the early steps in the pH-induced conformational**
1236 **conversion of the prion protein.** *Proc Natl Acad Sci USA*
1237 2001, **98**:2985-2989.
- 1238 MD simulations of PrP^c at neutral and low pH were used to probe
1239 the early steps in the conformational transition. The study shows
1240 that it is necessary to simulate conformational fluctuations under a
1241 variety of external conditions to obtain insights into the nature of
1242 events in the transition from PrP^c to PrP^{sc}.
- 1243 46. Swietnicki W, Petersen R, Gambetti P, Surewicz WK: **pH-**
1244 **dependent stability and conformation of the recombinant**
1245 **human prion protein PrP(90-231).** *J Biol Chem* 1997,
1246 **272**:27517-27520.
- 1247 47. Hornemann S, Glockshuber R: **A scrapie-like unfolding**
1248 **intermediate of the prion protein domain PrP(121-231)**
1249 **induced by acidic pH.** *Proc Natl Acad Sci USA* 1998,
1250 **95**:6010-6014.
- 1251 ••48. Kuwata K, Li H, Yamada H, Legname G, Prusiner SB,
1252 Akasaka K, James TL: **Locally disordered conformer of the**
1253 **hamster prion protein: a crucial intermediate to PrP^{sc}?**
1254 *Biochemistry* 2002, **41**:12277-12283.
- 1255 Using two-dimensional NMR measurements at various pressures
1256 on Syrian hamster PrP^c (90-231), the authors propose that, in the
1257 amyloidogenic intermediate PrP^{sc}, regions of helices 2 and 3 are
1258 disordered. Their key finding that helices 2 and 3 are implicated in
1259 the PrP^c \rightarrow PrP^{sc} transition is in accord with previous theoretical
1260 predictions [31**,32**].
- 1261 49. Lorimer GH: **A quantitative assessment of the role of the**
1262 **chaperonin proteins in protein folding *in vivo*.** *FASEB J*
1263 1996, **10**:5-9.
- 1264 50. Anfinsen CB: **Principles that govern the folding of protein**
1265 **chains.** *Science* 1973, **181**:223-230.
- 1266 51. Otzen DE, Oliveberg M: **Salt-induced detour through**
1267 **compact regions of the protein folding landscape.** *Proc*
1268 *Natl Acad Sci USA* 1999, **96**:11746-11751.
- 1269 ••52. Otzen DE, Kristensen O, Oliveberg M: **Designed**
1270 **protein tetramer zipped together with a hydrophobic**
1271 **Alzheimer homology: a structural clue to amyloid**
1272 **assembly.** *Proc Natl Acad Sci USA* 2000, **97**:9907-9912.
- 1273 This is the first study that used mutational analysis to investigate
1274 the factors that prevent wild-type S6 from aggregation. The
1275 experiments were used to introduce a key idea – natural proteins
1276 use charged gatekeeper residues (ones that are not involved in
1277 directing the folding process) to prevent intermolecular
1278 association.
- 1279 ••53. Perutz MF, Finch JT, Berriman J, Lesk A: **Amyloid fibers**
1280 **are water-filled nanotubes.** *Proc Natl Acad Sci USA* 2002,
1281 **99**:5591-5595.
- 1282 Using available experimental data and novel modeling methods,
1283 this study suggests that amyloid fibrils may have a near 'universal'
1284 structure.
- 1285 54. McDonald I, Thornton JM: **Satisfying hydrogen bonding**
1286 **potential in proteins.** *J Mol Biol* 1994, **238**:777-793.
- 1287 ••55. Sadqi M, Hernandez F, Pan UM, Perez M, Schaeberle
1288 MD, Avila J, Munoz V: **Alpha-helix structure in Alzheimer's**
1289 **disease aggregates of tau-protein.** *Biochemistry* 2002,
1290 **41**:7150-7155.
- 1291 This study challenges the commonly held belief that all amyloid
1292 fibrils comprise β -sheet structures. Using CD and FTIR
1293 spectroscopy, the authors suggest that, in the PHFs, the tau
1294 protein adopts an α -helical conformation.

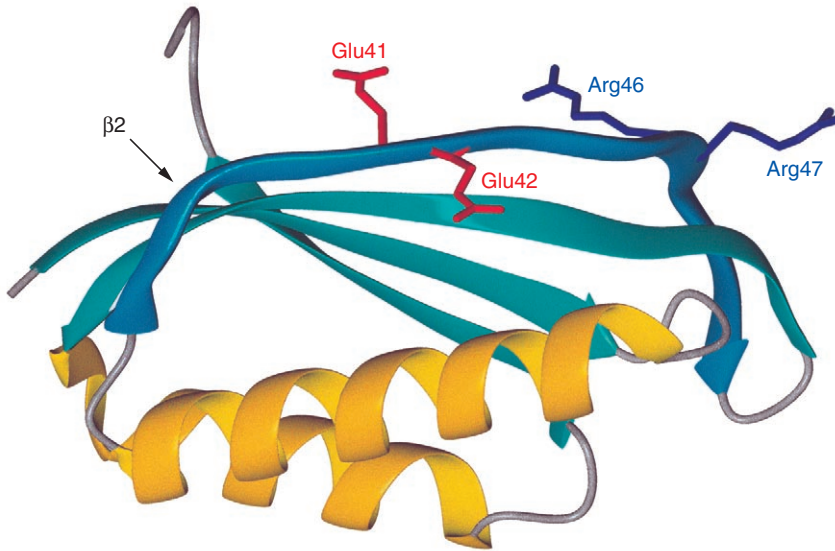
- 1295 ●56. Dima RI, Thirumalai D: **Exploring protein aggregation**
1296 **and self-propagation using lattice models: phase**
1297 **diagram and kinetics.** *Protein Sci* 2002, **11**:1036-1049.
1298 The authors use lattice models to describe various scenarios for
1299 protein aggregation. They use a toy model to verify the templated
1300 aggregation model for prion propagation [77].
- 1301 ●57. Wang W, Hecht MH: **Rationally designed mutations**
1302 **convert *de novo* amyloid-like fibrils into monomeric β -**
1303 **sheet proteins.** *Proc Natl Acad Sci USA* 2002, **99**:2760-
1304 2765.
1305 The authors show that inserting lysine in the middle of an
1306 alternating sequence of hydrophobic and hydrophilic residues
1307 results in soluble β -sheet proteins. This study provides direct
1308 experimental support to the ideas developed in [33**].
- 1309 ●58. Serag AA, Altenbach C, Gingery M, Hubbell WL,
1310 Yeates TO: **Arrangement of subunits and ordering of β -**
1311 **strands in an amyloid sheet.** *Nat Struct Biol* 2002, **9**:734-
1312 739.
1313 Using EPR, the authors propose a model for TTR fibrils. The
1314 rationale for this model follows from a combination of ideas
1315 presented in [33**,59].
- 1316 59. Klimov DK, Thirumalai D: **Native topology determines**
1317 **force-induced unfolding pathways in globular proteins.**
1318 *Proc Natl Acad Sci USA* 2000, **97**:7254-7259.
1319 60. West MW, Wang W, Patterson J, Mancias JD, Beasley JR,
1320 Hecht MH: ***De novo* amyloid proteins from designed**
1321 **combinatorial libraries.** *Proc Natl Acad Sci USA* 1999,
1322 **96**:11211-11216.
1323 61. Schwartz R, Istrail S, King J: **Frequencies of amino acid**
1324 **string in globular protein sequences indicate suppression**
1325 **of blocks of consecutive hydrophobic residues.** *Protein*
1326 *Sci* 2001, **10**:1023-1031.
1327 62. Rost B, Sander C: **Prediction of protein secondary**
1328 **structure at better than 70% accuracy.** *J Mol Biol* 1993,
1329 **232**:584-599.
1330 63. Bairoch A, Apweiler R: **The SWISS-PROT protein**
1331 **sequence database and its supplement TrEMBL in 2000.**
1332 *Nucleic Acid Res* 2000, **28**:275-284.
1333 64. Chou PY, Fasman GD: **Empirical predictions of protein**
1334 **conformation.** *Annu Rev Biochem* 1978, **47**:251-276.
1335 65. Moore RC, Lee IY, Silverman GL, Harrison PM, Strome R,
1336 Heinrich C, Karunaratne A, Pasternak SH, Chishti MA, Liang
1337 Y *et al.*: **Ataxia in prion protein (PrP)-deficient mice is**
1338 **associated with upregulation of the novel PrP-like protein**
1339 **Doppel.** *J Mol Biol* 1999, **292**:797-817.
1340 66. Nishida N, Tremblay P, Sugimoto T, Shigematsu K, Shirabe
1341 S, Petromilli C, Erpel SP, Nakaoko R, Atarashi R, Houtani T *et*
1342 *al.*: **A mouse prion protein transgene rescues mice**
1343 **deficient for the prion protein gene from Purkinje cell**
1344 **degeneration and demyelination.** *Lab Invest* 1999, **79**:689-
1345 697.
1346 67. Mo H, Moore RC, Cohen FE, Westaway D, Prusiner SB,
1347 Wright PE, Dyson HJ: **Two different neurodegenerative**
1348 **diseases caused by proteins with similar structures.** *Proc*
1349 *Natl Acad Sci USA* 2001, **98**:2352-2357.
1350 68. Hooft RWW, Vriend G, Sander C: **Errors in protein**
1351 **structures.** *Nature* 1996, **381**:272-273.
1352 ●69. Knaus KJ, Morillas M, Swietnicki W, Malone M,
1353 Surewicz WK, Yee VC: **Crystal structure of the human**
1354 **prion protein reveals a mechanism for oligomerization.**
1355 *Nat Struct Biol* 2001, **8**:770-774.
1356 The first crystal structure of a dimer of human prion protein is
1357 reported at 2 Å resolution. This structure, which may be a building
1358 block for PrP^{Sc}, shows that the dimer forms by a domain-swap
1359 mechanism.
- 1360 70. Liu Y, Gotte G, Libonati M, Eisenberg D: **A domain-**
1361 **swapped RNase A dimer with implications for amyloid**
1362 **formation.** *Nat Struct Biol* 2002, **8**:211-214.
- 1363 ●71. Petkova AT, Ishii Y, Balbach JJ, Antzutkin ON, Leapman
1364 RD, Delaglio F, Tycko R: **A structural model for Alzheimer's**
1365 **β -amyloid fibrils based on experimental constraints from**
1366 **solid state NMR.** *Biophys J* 2003, in press.
1367 A novel structural model for the A β ₁₋₄₀ amyloid fibril is proposed
1368 using solid-state NMR constraints. The authors showed that the
1369 number of salt bridges and hydrophobic interactions can be
1370 maximized by introducing a bend in each peptide (see also [27**]).
- 1371 72. Benzinger T, Gregory DM, Burkoth TS, Miller-Auer H, Lynn
1372 DG, Botto RE, Meredith SC: **Propagating structure of**
1373 **Alzheimer's β -amyloid₁₀₋₃₅ is parallel β -sheet with**
1374 **residues in exact order.** *Proc Natl Acad Sci USA* 1998,
1375 **95**:13407-13412.
1376 73. Balbach JJ, Ishii Y, Antzutkin ON, Leapman RD, Rizzo NW,
1377 Dyda F, Reed J, Tycko R: **Amyloid fibril formation by A β ₁₆₋₂₂**
1378 **a seven-residue fragment of the Alzheimer's β -amyloid**
1379 **peptide, and structural characterization by solid state**
1380 **NMR.** *Biochemistry* 2000, **39**:13748-13759.
1381 74. Ma B, Nussinov R: **Molecular dynamics simulations of**
1382 **alanine rich β -sheet oligomers: insight into amyloid**
1383 **formation.** *Protein Sci* 2002, **11**:2335-2350.
1384 75. Schweer O, Schonbrunn-Hanebeck E, Marx A, Mandelkow E:
1385 **Structural studies of tau protein and Alzheimer paired**
1386 **helical filaments show no evidence for beta-structure.** *J*
1387 *Biol Chem* 1994, **269**:24290-24297.
1388 ●76. Goux WJ: **The conformations of filamentous and soluble**
1389 **tau associated with Alzheimer paired helical filaments.**
1390 *Biochemistry* 2002, **41**:13798-13806.
1391 Extensive investigation of the structure of the PHFs further
1392 confirms the conclusions reached in [55**].
- 1393 77. Griffith JS: **Self-replication and scrapie.** *Nature* 1967,
1394 **215**:1043-1044.
1395 78. Harrison PM, Chan HS, Prusiner SB, Cohen FE:
1396 **Conformational propagation with prion-like**
1397 **characteristics in a simple model of protein folding.**
1398 *Protein Sci* 2001, **10**:819-835.
1399 ●79. Massi F, Straub JE: **Energy landscape theory for**
1400 **Alzheimer's amyloid β -peptide fibril elongation.** *Proteins*
1401 2001, **42**:217-229.
1402 The authors have proposed several schemes for the kinetics of
1403 fibril formation by A β peptides. By using the analogy with the
1404 energy landscape perspective of protein folding, many new
1405 predictions are made for the assembly of amyloid fibrils.
- 1406 ●80. Baskakov IV, Legname G, Prusiner SB, Cohen FE: **Folding**
1407 **of prion protein to its native α -helical conformation is**
1408 **under kinetic control.** *J Biol Chem* 2001, **276**:19687-
1409 19690.
1410 It is shown that PrP^c may be metastable, which suggests that the
1411 rarity of prion disorders is associated with a large barrier
1412 separating PrP^c and PrP^{Sc}. This study also implies that the kinetics
1413 of PrP^c formation follows scenario II (Figure 4).
- 1414 ●81. Serio TR, Cashikar AG, Kowal AS, Sawicki GJ, Moslehi
1415 JJ, Serpell L, Arnsdorf MF, Lindquist SL: **Nucleated**
1416 **conformational conversion and the replication of**
1417 **conformational information by a prion determinant.**
1418 *Science* 2000, **289**:1317-1321.
1419 Based on the kinetics of [PSI⁺] production from Sup35 in *S.*
1420 *cerevisiae*, the authors proposed a novel model that incorporate
1421 elements of the templated assembly and nucleation-growth
1422 mechanisms. It is likely that recent studies on A β aggregation
1423 provide additional examples of the NCC model.
- 1424 82. Ramirez-Alvarado M, Merkel JS, Regan L: **A systematic**
1425 **exploration of the influence of the protein stability on**
1426 **amyloid fibril formation *in vitro*.** *Proc Natl Acad Sci USA*
1427 2000, **97**:8979-8984.
1428 83. Eaton WA, Hofrichter J: **The biophysics of sickle cell**
1429 **hydroxyurea therapy.** *Science* 1995, **268**:1142-1143.

1430 84. Kraulis PJ: **MOLSCRIPT: a program to produce both** 1438 **and A β 42 oligomerize through distinct pathways.** *Proc*
1431 **detailed and schematic plots of protein structures.** *J Appl* 1439 *Natl Acad Sci USA* 2003, **100**:330-335.
1432 *Crystallogr* 1991, **24**:946-950. 1440 87. Hammarstrom P, Wiseman RL, Powers ET, Kelly JW:
1433 85. Koradi R, Billeter M, Wuthrich K: **Molmol: a program for** 1441 **Prevention of transthyretin amyloid disease by changing**
1434 **display and analysis of macromolecular structures.** *J Mol* 1442 **protein misfolding energetics.** *Science* 2003, **299**:713-
1435 *Graph* 1996, **14**:51-55. 1443 716.
1436 86. Bitan G, Kirkitadze MA, Lomakin A, Vollers SS, Benedeck
1437 GB, Teplow DB: **Amyloid β -protein (A β) assembly: A β 40**
1444



Current Opinion in Structural Biology

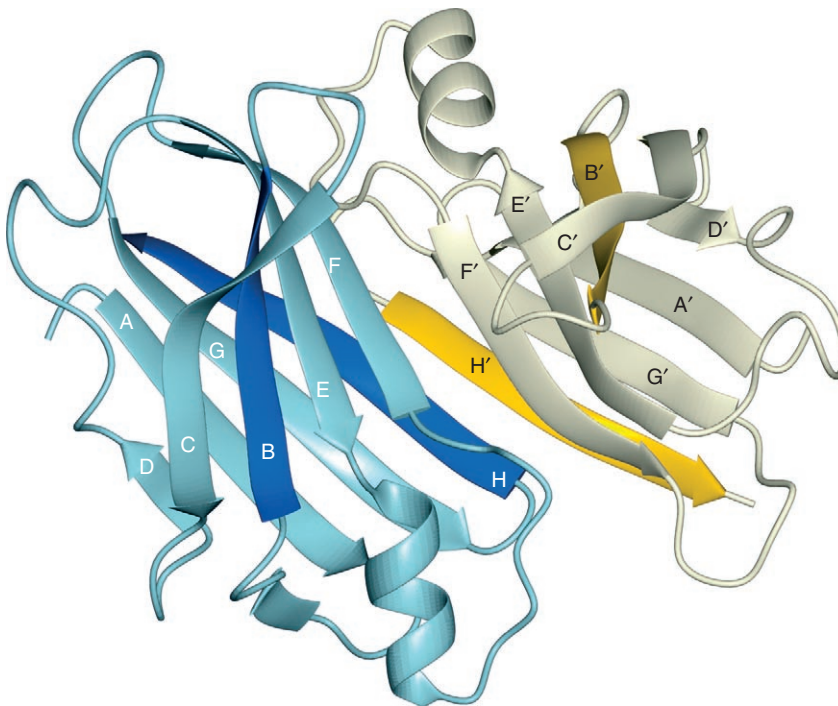
1445 **Figure 1**
1446
1447 (a) NMR structure of mouse PrP^{Sc} (PDB code 1ag2). Various measures of frustration (see text) between the sequence and its native three-
1448 dimensional structure show that at least the second half of helix 2 (H2) and part of the first half of helix 3 (H3) (colored in blue) are frustrated in the
1449 helical state. These regions, together with the disordered N-terminal segments, are implicated in the transition from PrP^{Sc} to the assembly-
1450 competent structure PrP^{Sc*}. (b) Solution structure of mouse Dpl (PDB code 1i17). Despite the similarity of the two structures, no frustrated region
1451 is found in Dpl. This may explain the absence of the scrapie form in Doppel. The figures were produced with the program Molscrip [84].
1452



Current Opinion in Structural Biology

Figure 2

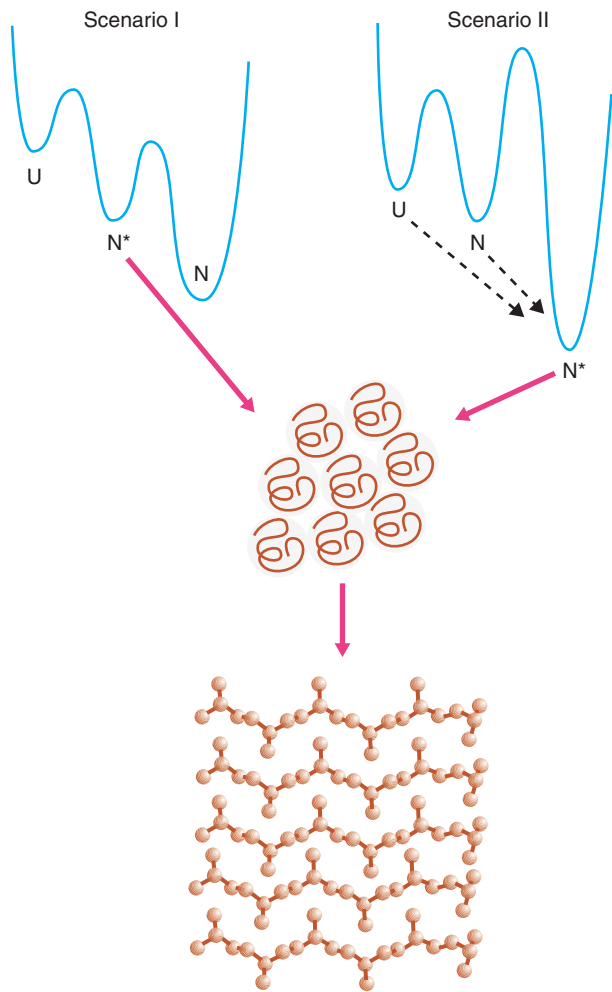
Ribbon diagram of the native structure of S6 (PDB code 1lou), which contains a single β sheet and two α helices. According to the OR^2 rule, β_2 , which is the edge strand (shown in blue), is protected against fibrillization by a combination of two mechanisms. The first one, based on electrostatic considerations, is enabled by the presence of two pairs of consecutive like charges (E41/E42 and R46/R47). Protection against aggregation in the second mechanism is afforded by the presence of a sharp twist and bend near the second pair of charged residues. Deletion of the pairs of charged residues by the double mutations E41A/E42A and R46M/R47M creates the mutant S6-Alz, which is prone to tetramerization. The figure was produced using MolMol [85].



Current Opinion in Structural Biology

Figure 3

The native dimeric assembly of TTR protein, which consists of β sheets CBEFF'E'B'C' and DAGHH'G'A'D'. Experiments by Yeates and co-workers [58**] suggest that the first β sheet in the dimer turns into the elementary building block of the fibril by unfolding strands C and D (C' and D'), and exposing the amyloidogenic strands B and B'. We also argue that the second β sheet (except D,D') is likely to be preserved in fibrils because of the strong interactions within the HH' interface. Protection of the strand B by short and twisted edge strands C and D is achieved by one of the aggregation-blocking mechanisms envisioned by R^2 . The figure was produced using MolMol [85].



1470
 1471
 1472
 1473
 1474
 1475

Figure 4

Schematic diagram of the two plausible scenarios of fibrillization based on the free energy landscape perspective. According to scenario I, the assembly-competent state N^* is metastable with respect to the monomeric native state N and is formed through partial unfolding. In scenario II, N^* is formed upon structural conversion either of the native state N (as in prions) or directly from the unfolded state U (as in $A\beta$ amyloid peptides). In both cases, proteins (or peptides) in N^* states must coalesce into larger oligomers capable of growth into fibrils.